Internal Rotation and Conformational Preferences in 1,2-Diaryl Derivatives of 1,1,2,2-Tetrachloroethane: a 1H DNMR and X-Ray Structural Study

Luciano Antolini, Ugo Folli, Adele Mucci, Silvia Sbardellati and Ferdinando Taddei
Dipartimento di Chimica, Università, Via Campi 183, 41100 Modena, Italy

The title compounds show in their 1H NMR spectra recorded at room temperature signals of different line-width characteristic of molecules with slow internal rotation around sterically crowded single bonds. From the DNMR study in [2H6]acetone solution of the 4,4'- (compound 1) and 3,3'-bis(benzoic acid) dimethyl ester (compound 2) and of the 3,3'-bispyridine (compound 3) derivative the dynamic parameters of two internal rotation processes, with different energies of activation, were extracted. The internal rotation process with higher energy barrier ($\Delta G^* = 13\text{--}14$ kcal mol^{-1}) was assigned to the *anti* $\rightleftharpoons$ *gauche* conformer interconversion, and that with lower energy barrier ($\Delta G^* = 8\text{--}9$ kcal mol^{-1}) to the rotation of aromatic rings around the C(sp^3)–C(sp^2) bond in the *gauche* conformer. The conformer populations measured at low temperature showed that the *gauche* conformer is the more abundant. The structural features of the conformers of compounds 1–3 were also investigated theoretically at a semi-empirical level with the AM1/MNDO method. The results of these calculations show that the *anti* conformer is the most stable one, yet the *gauche* form has higher polarity and this result could explain the increase of the *gauche* population in polar solvents. For compound 3 calculations were extended to the whole energy hypersurface having as coordinates the angles of rotation around the central C(sp^3)–C(sp^3) and C(sp^3)–C(sp^2) bonds. The theoretical free-energies of activation, even if largely underestimated, show that the barriers for the different internal processes follow the order: barrier for rotation around the C(sp^3)–C(sp^3) bond > barrier for rotation around the C(sp^3)–C(sp^2) bond in the *gauche* conformer > barrier for rotation around the C(sp^3)–C(sp^2) bond in the *anti* conformer. This order fits the trend of the first two barriers, experimentally determined. For compound 3 and for the 4,4'-bisbenzonitrile (compound 4) derivative, the crystal and molecular structure was obtained from X-ray analysis: the molecules have crystallographically dictated 1̄ symmetry with perfectly staggered *anti* conformation. Longer C–Cl bond lengths and smaller Cl–C–Cl bond angles than those present in structurally similar compounds indicate steric crowding around the C(sp^3)–C(sp^3) bond. Solid state conformations are in excellent agreement with the calculated ground-state rotational structure of these molecules.

Reductive coupling of PhCCl$_3$, induced by iron(II) chloride, occurs in polar solvents and anaerobic conditions and PhCCl$_2$CCl$_2$Ph is obtained in high yields.[1,2] This reaction has been tested in our laboratories[3] on a number of ring substituted benzotrichlorides and trichloromethylpyridines: *meta*- and *para*-phenyl substituted derivatives and 3-trichloromethylpyridine gave ArCCl$_2$CCl$_2$Ar derivatives as the main reaction product.

At room temperature, the 1H NMR spectra of these compounds showed signals of different line-width for the non-equivalent ring protons: those *ortho* to the –CCl$_2$– group are significantly broad. On lowering the sample temperature some of the signals, after further broadening, split up showing that freezing of internal motion has occurred.

The barrier for internal rotation of the CHCl$_2$ group in benzylidene dichloride is low,[4,5] yet is enhanced by the presence of *ortho*-substituents[6,7] and becomes measurable with the DNMR method. In 2,2,3,3-tetrachlorobutane the 1H NMR spectrum at 229 K showed[8] separate signals for the *anti* and *gauche* forms, the internal motion being frozen around the central C(2)–C(3) bond.

In the 1,2-diaryltetrachloroethanes two different processes of internal rotation should take place, namely that around the central C(sp^3)–C(sp^3) bond, process **I**, and that around the C(sp^3)–C(sp^2) bond, process **II**, the latter involving the correlated rotation of the two aromatic rings.

A number of questions thus arise concerning the dynamics

ArCl$_2$-C-Cl$_2$Ar

Process I

Ar-C-CCl$_2$CCl$_2$-C-Ar
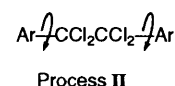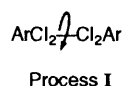
Process II

of the internal rotation in these molecules and the nature of the conformations involved: (i) whether the hindered internal motion observed at room temperature is associated with process **I** or process **II**; (ii) whether lowering of the sample temperature evidences the slowing down of the other process as well; (iii) once process **I** were found to have a higher energy barrier, whether the barrier for process **II** has equal or different values in the *anti*- and *gauche*-conformers; (iv) the degree of coupling existing between the two processes in the same molecule and, lastly, (v) the structure of the ground-state conformers involved in these rotational processes. We have thus undertaken the study of the dynamics of conformer interchange in molecules 1–3, by examining their 1H DNMR spectra in the temperature range allowed by the solvent where the solubility of the compounds was found to be satisfactory. The complexity of the conformational equilibria require that possible ground-state conformers be hypothesized, and quantum mechanical calculations were performed at a semi-empirical level. For the molecules which could be obtained in a suitable crystalline form, 3 and 4, the X-ray molecular structure was determined in order to have realistic molecular geometries in the solid state.
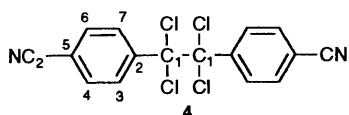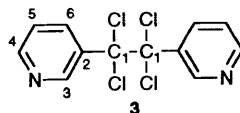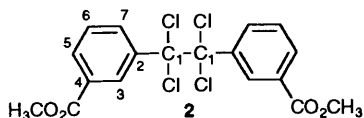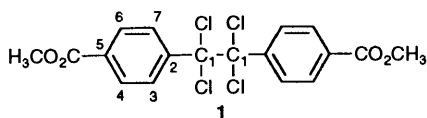
Experimental

General Procedures for the Synthesis of 1,2-*Diaryl*-1,1,2,2-*tetrachloroethanes.*—The appropriate aryltrichloromethane (10 mmol) was dissolved in CH_3CN (40 cm^3) (previously distilled from P_2O_5 under Ar atmosphere). Ar was continuously bubbled into the solution in order to obtain an inert atmosphere in the reaction apparatus. $FeCl_2 \cdot 4H_2O$ (30 mmol) was introduced and the mixture stirred for 7 h at 40–45 °C. The reaction was quenched by dilution with water followed by $CHCl_3$ extraction. The $CHCl_3$ solution was washed with water and dried ($MgSO_4$). An almost quantitative recovery of crude product was obtained after removal of the volatile materials. Purification was obtained by crystallization from CH_3CN, filtering the hot saturated solution from charcoal, with a recovery yield of 70–80%. In the case of the pyridine derivative, the reaction mixture, after dilution, was brought to pH 9–10, filtered through celite, thoroughly washing the precipitate and the filtrate with $CHCl_3$. The $CHCl_3$ solution was treated as before.

4,4′-(1,1,2,2-*Tetrachloroethane*-1,2-*diyl*)*bis*(*benzoic acid*) *dimethyl ester* (**1**). M.p. 240–243 °C (CH_3CN) (Found: C, 49.1; H, 3.0; $C_{18}H_{14}Cl_4O_4$ requires C, 49.6; H, 3.2%).

3,3′-(1,1,2,2-*Tetrachloroethane*-1,2-*diyl*)*bis*(*benzoic acid*) *dimethyl ester* (**2**). M.p. 144–146 °C (CH_3CN) (Found: C, 49.7; H, 3.2; $C_{18}H_{14}Cl_4O_4$ requires C, 49.6; H, 3.2%).

3,3′-(1,1,2,2-*Tetrachloroethane*-1,2-*diyl*)*bis*(*pyridine*)(**3**).M.p. 190–193 °C (CH_3CN) (Found: C, 44.6; H, 2.4; $C_{12}H_8Cl_4N_2$ requires C, 44.8; H, 2.5%).

4,4′-(1,1,2,2-*Tetrachloroethane*-1,2-*diyl*)*bis*(*benzonitrile*) (**4**). M.p. 264–267 °C (CH_3CN) (Found: C, 52.0; H, 2.1; $C_{18}H_8Cl_4N_2$ requires C, 51.9; H, 2.2%).

Crystal Data and X-Ray Structure Analysis.—Intensity data were collected on a CAD4 diffractometer, at room temperature, using graphite monochromated Mo-Kα radiation and the ω–2θ scan mode.

Compound **3**: $C_{12}H_8Cl_4N_2$, M = 322.02. Orthorhombic, a = 7.093(1), b = 13.529(1), c = 13.097(1) Å, V = 1256.8(3) Å^3 (by least-squares refinement on diffractometer angles for 25 automatically centred reflections, λ = 0.710 69 Å), space group *Cmca* ($n°$ 64), Z = 4, D_x = 1.702 g cm^{-3}, $F(000)$ = 648. Colourless, air stable prisms. Crystal dimensions 0.33 × 0.30 × 0.28 mm, μ(Mo-Kα) = 8.4 cm^{-1}.

For data collection ω scan width was (0.65 + 0.35 tan θ)°, ω scan speed 1.0–5.5° min^{-1}. Of 1092 measured reflections $(2 \leqslant \theta \leqslant 28°)$ 894 had $I \geqslant 3\sigma(I)$ and 673 were unique $(R_{int} = 0.015)$ and were used in the structure analysis. An empirical absorption correction based on the ψ scan,[9] was applied to intensities $(0.966 \leqslant T_{factor} \leqslant 0.999)$. Systematic extinctions were consistent with *Cmca* and *Aba*2 space groups. The centrosymmetric *Cmca* space group was assumed on the basis of statistical tests, which favour the former possibility, and was verified by successful solution and refinement of the structure.

The structure was solved by direct methods (SHELX86),[10] and refined through full-matrix least-squares calculations (SHELX76).[11] Only the Cl atom was found to have full site occupancy factor (s.o.f.). All other atoms were assumed to be equally distributed over two close positions related by twofold axis [C(2)] or mirror plane (pyridine group), hence with s.o.f. = 0.5, as required by Z = 4. Non-H atoms were refined anisotropically, but with B_{ij} constraints of atoms lying on a mirror plane applied to C and N atoms; H atoms located in ΔF maps, were refined isotropically with a common temperature factor. The weighting scheme w = $1.0/[\sigma^2(F_o) + 0.000\,85F_o^2)]$, with $\sigma(F_o)$ from counting statistics, gave satisfactory agreement analyses. Final R and R_w values are 0.022 and 0.025.

Attempts were made to refine the structure with the reduced symmetry constraints of space group *Aba*2. However, higher reliability indices (R = 0.026, R_w = 0.027) and unrealistic deviations from coplanarity of atoms belonging to the pyridine ring proved that our space group choice was justified. A drawing of the disorder model is available from the authors.

Compound **4**: $C_{16}H_8Cl_4N_2$, M = 370.06. Monoclinic, a = 10.731(2), b = 6.913(1), c = 11.396(2) Å, β = 108.32(2)°, V = 802.6(8) Å^3 (by least-squares refinement on diffractometer angles of 25 automatically centred reflections, λ = 0.710 69 Å), space group $P2_1/a$ ($n°$ 14), Z = 2, D_x = 1.531 g cm^{-3}, $F(000)$ = 372. Colourless, air stable plates. Crystal dimensions 0.36 × 0.28 × 0.08 mm, μ(Mo-Kα) = 6.65 cm^{-1}.

For data collection ω scan width was (0.65 = 0.35 tan θ)°, ω scan speed 0.87–5.5° min^{-1}. Of 2020 measured reflections $(2 \leqslant \theta \leqslant 28°)$, 1536 had $I \geqslant 3\sigma(I)$, and 1364 were unique $(R_{int} = 0.012)$, and were used after absorption correction based on empirical ψ scan[9] $(0.853 \leqslant T_{factor} \leqslant 0.999)$, in the structure analysis.

The structure was solved by direct methods (SHELX86),[10] and refined through full-matrix least-squares calculations (SHELX76).[11] All non-hydrogen atoms were treated anisotropically, and hydrogens, located in ΔF maps, isotropically. The weighting scheme w = $1.0/[\sigma^2(F_o + 0.000\,85F_o^2)]$ gave satisfactory agreement analyses. Final R and R_w values are 0.029 and 0.033, respectively.

Scattering factors were from SHELX76.[11] Most of the calculations were carried out on a VAX 6310 computer. Tables of final fractional coordinates and full lists of bond distances and bond angles have been deposited at the Cambridge Crystallographic Data Centre.*

NMR Measurements.—^{1}H NMR spectra were recorded at 400.13 MHz on a Bruker AMX-400 spectrometer equipped with computer controlled variable temperature unit (accuracy ± 1 K) in 5 mm probes. [$^2H_6$]Acetone solutions (~0.05 mol dm^{-3}) and, for compounds **2** and **3** also [^2H]chloroform solutions (~0.01 mol dm^{-3}) were employed. For compound **3** these concentrations were close to the saturation limit. Spectral parameters are: pulse width 90°, acquisition time *ca.* 4 s,

---

Table 1 ¹H Chemical shifts[a] (δ) and molar fraction (n_A) of the *anti* conformer for compounds 1-4 measured in [²H₆]acetone solution at 250 K

Compound	n_A	H-3		H-4/Me-4		H-5/Me-5		H-6		H-7	
		A	G	A	G	A	G	A	G	A	G
1	0.19	8.42	7.65	8.31	8.06	4.08	4.04	8.31	8.06	8.42	7.65
2	0.20 (0.30)[b]	8.72	7.71	3.94	3.81	8.19	8.09	7.74	7.52	8.39	7.70
3	0.36 (0.44)[b]	9.23	8.43	8.74	8.65	7.63	7.42	8.49	7.76		
4	0.29	8.36	7.61	8.06	7.83			8.06	7.83	8.36	7.61

[a] A and G refer to the *anti* and *gauche* conformers. [b] In [²H]chloroform solution.

Table 2 ¹H Chemical shifts (δ) for the ground-state conformers generated in the internal rotation around the C(1)–C(2) bond in the *gauche* conformer of compounds 1–3 ([²H₆]acetone solution) at 250 K

Compound	H-3	H-4/Me-4	H-5/Me-5	H-6	H-7
1[a]	8.43 6.85	8.35 7.89	4.02	7.89 8.35	6.85 8.43
2[b]	8.64 6.98 6.71	3.90 3.66 3.64	8.11	7.28 7.78	6.78 8.40
3[b]	9.22 7.67	8.70	7.31 7.67	6.98 8.54	

[a] $T = 190.0$ K. [b] $T = 178.3$ K.

number of scans selected in order to obtain a good signal to noise ratio. Chemical shifts (δ) are given relative to TMS.

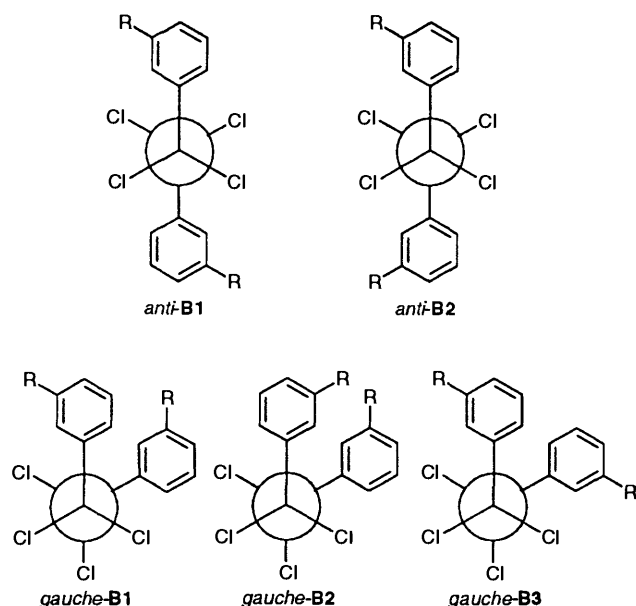Calculations relative to the theoretical methods were performed on a IBM AIX/RS6000 computer.

Results

¹H DNMR Spectra.—The ¹H NMR spectra of compounds 1–4 were run in [²H₆]acetone, since this solvent provides conditions of moderately good solubility and is amenable to being employed in a fairly wide temperature interval (178–329 K). At room temperature (298 K), the spectra show signals with different band-width, and a marked temperature dependence in the range where they could be obtained in the solvent employed. The presence in these molecules of at least two hindered processes of internal rotation is evident from the behaviour of the DNMR spectra. In fact, on lowering the sample temperature to 240–250 K the spectra of two chemical species appear, which can be assigned to the *anti* and *gauche*

anti-B1   *anti*-B2

gauche-B1   *gauche*-B2   *gauche*-B3

Scheme 1 Preferred molecular conformations for the internal rotation process around the C(sp³)–C(sp³) and C(sp³)–C(sp²) bonds in compounds 1–3 (in compound 1 R = H, only one form exists for the *anti* and *gauche* conformations; for compound 3, R is the ring nitrogen)

conformers, one in a larger amount than the other. When the temperature is further lowered, the signals of the more abundant conformer give rise to a splitting in two groups, passing through coalescence.

In Table 1 the ¹H chemical shifts assigned to the *anti* and *gauche* conformers of compounds 1–3 and their conformer population are reported. The chemical shifts of the conformer present in larger amount, which we will provisionally assign to the *gauche* conformer, are systematically at higher field with respect to those of the other conformer and the chemical shift difference decreases for *ortho*, *meta* and *para* protons (positions referred to the –CCl₂– substituent) in that order. A shift to higher field is expected in the *gauche*, with respect to the *anti*, form owing to the orientation of the aromatic rings which should exert a reciprocal screening effect (high-field shift due to ring currents). For temperatures lower than 250 K the signals of the *gauche* conformer show splittings due to the 'freezing' of conformational freedom around the C(sp³)–C(sp²) bond(s) and the values measured below 190 K are reported in Table 2. For the majority of the protons, at least two separate multiplets appear, yet for H-5 of compound 2 and H-4 of compound 3 the line-width is greater than that of the *anti* conformer. Compounds 1 and 3 show two groups of signals which contain the same number of protons, yet, for compound 2, a higher number of multiplets than expected for two conformers is monitored on lowering the sample temperature below 185 K.

The ¹H DNMR spectra, recorded for compounds 1–3, were processed in order to extract the dynamic features of the conformational exchange. Total-line shape analysis was performed with the DNMR3 [12] and DNMR5 [13,14] software. The two rotational processes were treated as totally uncoupled. This is not completely correct, since in the temperature interval where the first rotational process is almost frozen the second process becomes responsible for band broadening. On the other hand a simultaneous treatment of the two processes is outside the capacity of the software we have employed for line-shape simulation. The T_2 values at different temperatures were obtained from line-width changes of a signal not involved in proton exchange. The simulated band-shapes were obtained either with fixed populations, those measured at 240–250 K, and assuming temperature dependence. The results from the two approaches do not significantly differ and the ratio of the conformer populations seems not to change appreciably with temperature. The chemical shifts showed drifts with temperature changes (important for H-5 of the *anti* conformer of compound 3, -0.4 Hz K⁻¹) and this was accounted for in band-shape simulation, even if it was not feasible for all the protons. The signals of H-3 and H-7 of the *gauche* conformer of compound 2, for example, overlap and are broad in the temperature range examined. Tentative values were employed in these cases and the resulting shape of the calculated spectrum more similar to the experimental one (by direct inspection) was adopted. Whenever possible, the rate constants were derived from the simulation of aromatic protons since the singlet structure of the methyl group has a lower sensitivity [14] to the optimization of the parameters (chemical shifts and populations) at temperatures different from that of coalescence. Nevertheless, the

Table 3 Thermodynamic parameters for the *anti* $\rightleftharpoons$ *gauche* equilibrium in compounds 1–3 in [^{2}H$_6$]acetone solution at 298 K

Compound	$A/10^{14}$	$E_a{}^a$	r^b	ΔH^{*a}	ΔS^{*c}	ΔG^{*a}
1	1.3 ± 0.4	15.3 ± 0.2	0.9994	14.7 ± 0.4	4.0 ± 0.6	13.5 ± 0.6
2	0.9 ± 0.5	15.3 ± 0.2	0.9987	14.7 ± 0.3	3.0 ± 1.0	13.7 ± 0.6
3	0.8 ± 0.2	15.3 ± 0.2	0.9995	14.7 ± 0.4	3.0 ± 0.6	13.8 ± 0.6

^{a} In units of kcal mol^{-1} (1 kcal mol^{-1} = 4.184 kJ mol^{-1}). ^{b} Bravais–Pearson coefficient of the Arrhenius plot. ^{c} In units of cal mol^{-1} K^{-1}.

Table 4 Thermodynamic parameters for the rotational process of the aromatic ring [around the C(sp^3)–C(sp^2) bond] in compounds 1–3, in [^{2}H$_6$]acetone solution at 298 K

Compound	$A/10^{14}$	$E_a{}^a$	r^b	ΔH^{*a}	ΔS^{*c}	ΔG^{*a}
1	5 ± 2	10.7 ± 0.2	0.9990	10.1 ± 0.4	6.6 ± 0.8	8.2 ± 0.7
2^d	7 ± 5	11.2 ± 0.3	0.9982	10.6 ± 0.3	7 ± 1	8.4 ± 0.7
	0.2 ± 0.1	9.7 ± 0.1	0.9992	9.1 ± 0.5	0.5 ± 0.7	9.0 ± 0.7
3^e	0.4 ± 0.1	9.2 ± 0.1	0.9996	8.6 ± 0.5	1.4 ± 0.4	8.2 ± 0.6

^{a} In units of kcal mol^{-1}. ^{b} Bravais–Pearson coefficient of the Arrhenius plot. ^{c} In units of cal mol^{-1} K^{-1}. ^{d} The first line refers to the line-shape simulation of the methyl group (DNMR5 software with a three-site exchange model) and the second to the line-shape simulation of the aromatic protons (DNMR3 software) with a two-site exchange model. ^{e} With a two-sites line-shape simulation model (see text).

behaviour of the methyl signal of compound 1 was found to be more reliable within the temperature range (240–260 K) relevant for the study of process I, since not affected by the second rotational process.

Rate constants derived from line-shape simulation were fitted[15,16] to the Arrhenius equation and the dynamic parameters E_a, ΔH^*, ΔS^*, and ΔG^* were obtained with general methods[15] (Table 3). For compound 2 the k values obtained at temperatures below 270 K are affected by large errors and were not employed for deriving the dynamic parameters: for this compound the influence of process II becomes significant at temperatures higher than is the case with the other compounds and broadening of the signals of the *gauche* conformer occurs.

With regard to process II, internal rotation around the C(sp^3)–C(sp^2) bond, a complete line-shape treatment of the mutual exchange could be applied only to compound 1. For compounds 2 and 3, simulation of the line-shape of aromatic protons requires us to consider four nuclei exchanging between four sites, and the problem exceeds the dimensions of the DNMR3 and DNMR5 software. Moreover, the separation and resolution of the multiplets of the different protons is not satisfactory for accurate comparison of simulated and experimental spectra. For compounds 2 and 3 rate constants were derived from the signals of aromatic protons by assuming an exchange problem similar to that occurring in compound 1, that is to say, an exchange of four nuclei between two sites. The rate constant k obtained within this approximation is a combination of those, relative to different routes of conformer exchange, and is only an 'apparent' value. For compound 2 the dynamic parameters were obtained from rate constants derived by the methyl signal as well. The two sets of values, reported in Table 4, differ significantly: those obtained from the aromatic protons may be considered more reliable. The entropy of activation turns out to be much lower when derived from the aromatic protons: which of the two values is more correct is difficult to assess. Both values are probably affected by a large experimental error.

Crystal Structures.—Among the 1,2-diaryl-1,1,2,2-tetra-chloroethanes synthesized in our laboratories, compounds 3 and 4 were obtained in a crystalline form suitable for X-ray analysis. These compounds are deemed to be representative for the structure features of this class of molecules, at least of those compounds not bearing *ortho* substituents in the rings, which could modify their conformational pattern.

Drawings of the structures of compounds 3 and 4, showing the atom numbering schemes, are given in Figs. 1 and 2,
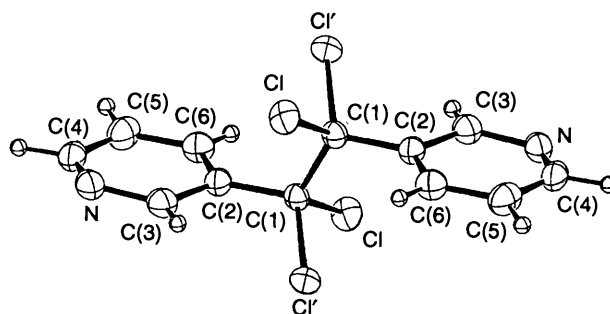

Fig. 1 ORTEP[17] drawing of the molecular structure of compound 3 with atom numbering scheme. Equivalent atoms are related by an inversion centre at the midpoint of the C(1)–C(1) bond; primed Cl atoms are related to unprimed by a twofold axis. Thermal ellipsoids enclose 50% probability.
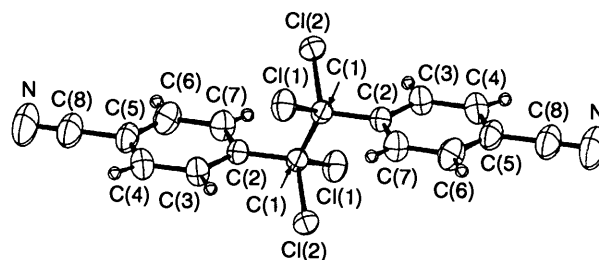

Fig. 2 Atom labelling and thermal ellipsoids (50%) for non-H atoms of compound 4. Equivalent atoms are related by an inversion centre at the midpoint of the C(1)–C(1) bond.

respectively. Selected bond distances, bond angles and torsional angles are reported in Tables 5 and 6.

The molecular conformation and dimensions of compounds 3 and 4 are very similar. Both molecules have crystallographically dictated $\bar{1}$ symmetry, and, around the C(1)–C(1) bond, show perfect staggering with aromatic rings *anti*. The planar C(2)–C(1)–C(1)–C(2) fragments and the aromatic rings are very nearly perpendicular with a dihedral angle of 88.7°, for both molecules. It is noteworthy that the same molecular conformation and symmetry requirement ($\bar{1}$) were previously observed[18] in 4,4′-(1,1,2,2-tetrachloroethane-1,2-diyl)bis-chlorobenzene. Up to now, this is the only structure determination of 1,1,2,2-tetrachloroethane derivatives of which we are aware. Good agreement with corresponding values of bond distances and angles of our compounds is found. Nevertheless some of these geometrical parameters differ significantly from those reported for many DDT-type

Table 5 Experimental bond-distances (Å), bond-angles (°) and torsion angles (°) determined by X-ray diffraction for compound 3[a]

Cl(1)–C(1)	1.806(3)	Cl''–C(1)	1.804(3)
C(1)–C(1')	1.558(4)	C(1)–C(2)	1.531(4)
C(2)–C(3)	1.380(4)	C(2)–C(6)	1.384(4)
C(3)–N	1.364(4)	N–C(4)	1.339(4)
C(4)–C(5)	1.373(5)	C(5)–C(6)	1.395(5)
C(1')–C(1)–Cl	107.4(2)	C(1')–C(1)–Cl''	107.6(2)
C(1')–C(1)–C(2)	115.2(2)	Cl''–C(1)–Cl	104.5(2)
Cl–C(1)–C(2)	110.9(2)	Cl'–C(1)–C(2)	110.7(2)
C(1)–C(2)–C(3)	120.7(3)	C(1)–C(2)–C(6)	121.3(3)
C(3)–C(2)–C(6)	118.0(3)	C(2)–C(3)–N	123.9(3)
C(3)–N–C(4)	115.6(3)	N–C(4)–C(5)	123.7(3)
C(4)–C(5)–C(6)	119.0(3)	C(5)–C(6)–C(2)	118.7(3)
Cl–C(1)–C(1')–Cl'	180	Cl–C(1)–C(1')–Cl^	−68.0(2)
Cl–C(1)–C(2)–C(3)	31.7(4)	Cl–C(1)–C(2)–C(6)	−147.0(3)
Cl''–C(1)–C(1')–Cl'	68.0(2)	Cl''–C(1)–C(1')–Cl^	180
Cl''–C(1)–C(2)–C(3)	147.2(3)	Cl''–C(1)–C(2)–C(6)	−31.6(4)
Cl'–C(1')–C(1)–C(2)	−56.0(3)	Cl'–C(1')–C(1)–C(2)	56.0(3)
C(1)–C(2)–C(3)–N	174.1(3)	C(1)–C(2)–C(6)–C(5)	−179.2(6)
C(1')–C(1)–C(2)–C(3)	−90.5(3)	C(1')–C(1)–C(2)–C(6)	90.7(4)
C(2)–C(3)–N–C(4)	11.6(5)	C(2)–C(6)–C(5)–C(4)	−2(1)
C(3)–C(2)–C(6)–C(5)	2.1(7)	C(3)–N–C(4)–C(5)	−11.7(8)
N–C(3)–C(2)–C(6)	−7.1(5)	N–C(4)–C(5)–C(6)	7(1)

[a] ' Symmetry transformation $1 - x$, $1 - y$, $1 - z$ of the reference coordinates. '' Symmetry transformation x, $1 - y$, $1 - z$ of the reference coordinates. ^Symmetry transformation $1 - x$, y, z of the reference coordinates.

Table 6 Experimental bond-distances (Å), bond-angles (°) and torsional angles (°) determined by X-ray diffraction for compound 4[a]

Cl(1)–C(1)	1.788(2)	Cl(2)–C(1)	1.790(2)
C(1)–C(1')	1.575(4)	C(1)–C(2)	1.529(3)
C(2)–C(3)	1.389(4)	C(2)–C(7)	1.388(3)
C(3)–C(4)	1.393(4)	C(4)–C(5)	1.382(4)
C(5)–C(6)	1.381(4)	C(5)–C(8)	1.447(4)
C(6)–C(7)	1.390(4)	C(8)–N	1.134(5)
Cl(1)–C(1)–Cl(2)	105.9(1)	Cl(1)–C(1)–C(1')	107.9(2)
Cl(2)–C(1)–C(1')	107.2(2)	Cl(1)–C(1)–C(2)	110.6(1)
Cl(2)–C(1)–C(2)	110.1(2)	C(1')–C(1)–C(2)	114.3(2)
C(1)–C(2)–C(3)	120.3(2)	C(1)–C(2)–C(7)	120.5(2)
C(3)–C(2)–C(7)	119.3(2)	C(2)–C(3)–C(4)	120.4(2)
C(3)–C(4)–C(5)	119.5(3)	C(4)–C(5)–C(6)	120.7(3)
C(4)–C(5)–C(8)	119.9(3)	C(6)–C(5)–C(8)	119.4(3)
C(5)–C(6)–C(7)	119.5(3)	C(6)–C(7)–C(2)	120.5(3)
N–C(8)–C(5)	179.7(3)		
Cl(1)–C(1)–C(2)–C(3)	−149.6(2)	Cl(1)–C(1)–C(2)–C(7)	31.1(2)
Cl(1)–C(1)–C(1')–Cl(1')	180	Cl(1)–C(1)–C(1')–Cl(2')	−66.1(2)
Cl(1)–C(1)–C(1')–C(2')	56.5(3)	Cl(2)–C(1)–C(2)–C(3)	−33.0(2)
Cl(2)–C(1)–C(2)–C(7)	147.8(2)	Cl(2)–C(1)–C(1')–Cl(1')	66.1(2)
Cl(2)–C(1)–C(1')–Cl(2')	180	Cl(2)–C(1)–C(1')–C(2')	−57.3(3)
C(1)–C(2)–C(3)–C(4)	−179.2(2)	C(1)–C(2)–C(7)–C(6)	179.5(2)
C(2)–C(3)–C(4)–C(5)	−0.5(3)	C(2)–C(7)–C(6)–C(5)	−0.1(4)
C(2)–C(1)–C(1')–Cl(1')	−56.5(3)	C(2)–C(1)–C(1')–Cl(2')	57.3(3)
C(2)–C(1)–C(1')–C(2')	180	C(3)–C(2)–C(7)–C(6)	0.3(3)
C(3)–C(4)–C(5)–C(6)	0.6(4)	C(3)–C(4)–C(5)–C(8)	−178.8(2)
C(3)–C(2)–C(1)–C(1')	88.4(3)	C(4)–C(3)–C(2)–C(7)	0.0(3)
C(4)–C(5)–C(6)–C(7)	−0.3(4)	C(7)–C(6)–C(5)–C(8)	179.1(2)
C(7)–C(2)–C(1)–C(1')	−90.9(3)		

[a] Primed atoms are related to unprimed ones by the symmetry transformation $1 - x$, $-y$, $-z$ of the reference coordinates.

derivatives of known structure[19] and from mean values retrieved from the Cambridge Crystallographic Database.[20] Bond distances Cl–C(sp³) of 1.806(3) and 1.804(3) Å in compound 3, 1.788(2) and 1.790(2) Å in 4, and the reported values of 1.792 and 1.793 Å in ref. 18 are all longer than the averaged value of 1.782 Å found in DDT-type derivatives.[19] Such bond-lengthening is accompanied by substantial decrease of Cl–C–Cl bond angles: their values of 104.5(2), 105.9(1) and 106.2° for 3, 4 and the p-chloroderivative,[18] respectively, are significantly lower than the ideal sp³ angle of 109.5°. Lengthening of the C(sp³)–C(sp³) and C(sp³)–C(sp²) bonds are also observed. The C(1)–C(1) distances range from 1.558(4) to

1.585(5) Å, and the C(1)–C(2) bonds from 1.529(4) to 1.531(4) Å, which compare with a mean value of 1.513 Å.[20] It is likely that not only the strong electron-withdrawing effect of the chlorine atoms, but also steric interactions between chlorines and ortho hydrogens of aryl groups, play a role in bond lengthening.

A few short van der Waals contacts are present in the crystal packing of compound 3; the shortest ones [3.135(3) and 3.313(3) Å] occur between the Cl atom and the pyridine nitrogen. This could probably account for an unexpected out-of-plane displacement (0.056 Å) of the N atom in the pyridine ring.

Likewise, only five non-bonded distances less than 3.60 Å are

Table 7 Populations of *anti* and *gauche* conformations (see **Scheme 1**) and weight-averaged dipole moments calculated with the AM1/MNDO method

| Compound | anti[a] | | gauche[a] | | | $n_A{}^b$ | $\mu_A{}^c$ | $n_G{}^b$ | $\mu_G{}^c$ |
	B1	**B2**	**B1**	**B2**	**B3**				
1	0.546			0.380		0.549	1.370	0.451	2.309
2	0.285	0.339	0.153	0.094	0.101	0.624	1.634	0.376	3.153
3	0.334	0.307	0.161	0.071	0.082	0.645	1.588	0.355	2.682
4	0.607			0.350		0.610	0.002	0.390	1.872

[a] Populations of the conformers with the aromatic ring parallel with the C(2)-C(1)-C(1)-C(2) plane are lower than 2% and are not reported. [b] Total conformer populations of *anti* and *gauche* type. [c] Weight-averaged dipole moments in Debye.

present in the molecular packing of compound **4**. The shortest separations are Cl(2)•••Cl(2) = 3.322(1) Å, and C(4)•••N = 3.440(5) Å.

Theoretical Results.—Conformational trends were analysed with a theoretical approach in order to obtain predictive information on the different internal rotational paths. The theoretical approach was carried out with the AM1/MNDO semi-empirical method,[21] previously tested[22] for predicting the features of rotational processes around single bonds in organic molecules. The method underestimates[22] rotational barriers and also the E/Z energy difference obtained is often too low, though the trend of rotational barriers and conformational preferences is satisfactorily reproduced for molecules with similar molecular constitution. On the other hand, it has recently been reported[23] that satisfactory descriptions of rotational barriers at an almost quantitative level in conjugated ethylenes and substituted benzenes can be obtained by MO *ab-initio* calculations with large AO basis sets (6-311G**) and at least second-order Moller-Plesset (MP2) perturbation theory. This level of calculations is almost prohibitive for the molecules here examined and we tried to predict, at a qualitative level, the trends of rotational processes around single bonds by employing the semi-empirical AM1/MNDO method.[24] A full investigation of critical points of the energy hypersurface was carried out only for compound **3**, where additional complications due to the conformations of ring substituents are not present. For compounds **1**, **2** and **4** only the rotational minima were studied; for compounds **1** and **2** all the possible orientations of the COOCH₃ group in these conformations were taken into account. Full geometry relaxation was performed in each conformational minimum.

From the energy of the conformations and their statistical weight the populations of the *anti* and *gauche* forms were calculated and the results are collected in Table 7, where the weight-averaged dipole moments of these conformations are also reported. Labelling of the conformations is as shown in Scheme 1: the conformations with the aromatic ring plane parallel with the C(2)-C(1)-C(1)-C(2) plane (labelled of A type) are of high energy and can be neglected.

Besides the approximate character of these calculations it is worth noting two peculiarities resulting from the comparison with experimental results which show that the trend is satisfactorily reproduced. In derivatives **1–4** the *anti* conformations of **B** type have lower energy content, in agreement with the X-ray molecular structure of compounds **3** and **4**. Furthermore, comparison of experimental and calculated geometry shows quite satisfactory reproduction of the most significant features of these molecules: differences from experimental values do not exceed 0.03 Å for bond lengths and 3° for bond angles. For compound **3** the most stable calculated conformation agrees with the solid state structure even in the relative orientation of the two heterocyclic nitrogen atoms [*anti*-B1].

Scanning of the AM1/MNDO energy hypersurface was

performed for compound **3**, by calculating energy values in 20° steps for rotations around the central C(sp³)-C(sp³) and the two C(sp³)-C(sp²) bonds while the other geometrical parameters were relaxed (flexible rotor approximation).[25] Potential energy maxima for rotation around the C(1)-C(1) bond were found for eclipsed forms: the one corresponding to the ring-ring eclipsed situation has higher energy. Small differences in these maxima also occur at different relative orientations of the heterocyclic nitrogen. With regard to rotation of the aromatic ring around the C(sp³)-C(sp²) bond, the lowest energy path requires that one pyridine ring remain in one almost constant orientation (oscillates within 30° around the conformation of minimum energy) and the rotation of the two rings can thus be considered not to occur simultaneously. The maxima were then characterized as saddle-points † in order to obtain the energy of the rotational transition state. Contributions from zero-point energy (ZPE) were also considered in order to calculate energy barriers ΔE^*. The calculated energy barriers for the *anti–gauche* equilibrium and for the internal rotation about the C-C bond in the *anti* and *gauche* conformers are, for compound **3** 7.9, 2.6 and 3.6 kcal mol⁻¹ respectively. Comparison with the experimental values of 15.3 and 9.2 kcal mol⁻¹ allows the assignment of the larger value to the *anti–gauche* equilibrium.

Discussion

The sequence of energy barriers from semi-empirical calculations in compound **3** shows that the rotational process occurring at higher temperature is process **I**. Owing to the large difference in energy barriers found for process **I** and process **II**, it is reasonable to suppose that the effect of substituents in *meta* and *para* positions is not able to reverse this order, which should thus be present in all the compounds examined. Evidence from NMR measurements is, accordingly, in favour of this process occurring at higher temperature in compounds **1–3**.

A second point needs, nevertheless, further consideration: the assignment of the barrier measured at lower temperature to process **II** in the *gauche* conformer. In order to reinforce this conclusion, it is necessary to confirm that the protons undergoing the observed exchange are those of the *gauche* conformer, and that the conformations of the aromatic ring are effectively of **B** type in solution, as occurs for the solid state conformation and as results from calculations on the free molecule. To this end, we notice that in compound **1**, the chemical shift differences of the magnetically non-equivalent *ortho* and *meta* protons in the *gauche* conformer (see Table 2) are 1.58 and 2.46 ppm, and those at lower field are close to the values measured for the *anti* conformer (see Table 1). The

---

† For calculating energy minima, saddle-point energy, zero-point energy and thermodynamic parameters, the AM1/MNDO option of the GAUSSIAN-92 software[26] was employed. For the ground-state conformations the relative energy content derived by employing this software and that of ref. 24 differs less than 0.01 kcal mol⁻¹.

protons at higher field of the *gauche* form should thus be those subjected to the screening effect of ring currents due to the other aromatic ring. Since the chemical shifts of the *ortho* and *meta* protons of the *anti* form have values very similar to those of the corresponding, less shielded protons of the *gauche* form, the orientation of **B** type should be the predominant one for the *anti* conformer and, as a very realistic consequence, also for the *gauche* conformer.

In compound **3** each of the *ortho* (referred to the –CCl$_2$– group) protons (H-3 and H-6) of the *gauche* conformer is split at low temperature (Table 2) and the chemical shift difference is close to that found in compound **1**. The same evidence exists for H-5, corresponding to the *meta* protons of compound **1**. This result suggests two possible conformational conclusions, *i.e.* that the *gauche* conformer is: (i) an equimolecular mixture of the **B2** and **B3** forms and (ii) a mixture of the three **B** forms with **B2** and **B3** in equal amounts. These conclusions assume that chemically equivalent protons have similar chemical shift values in the three forms. According to theoretical results (Table 7) the population of the **B1** form should be almost equal to the sum of those of **B2** and **B3**. The low temperature ^{1}H spectrum of compound **2** is more complex, yet three separate resonances can be assigned to H-3 and to the methyl group: of these, the two at higher field should belong to the **B1** and **B2** forms and that at lower field to the **B1** and **B3** forms. It should be remembered that in the **B1** form, H-3 and the CH$_3$ protons of the two aromatic rings are not chemically equivalent. The integrated area of the signal at lower field is nearly equal to the sum of those of the signals at higher field, and the three forms of the *gauche* conformation should have almost the same energy content. Approximately, this is also the conclusion reached from the theoretical approach.

The thermodynamic parameters relative to the conformer interchange processes show that an energy difference of nearly 5 kcal mol^{-1} differentiates the transition rotational states of process **I** with respect to process **II** in compounds **1–3**. The values of the activation energy (enthalpy or free-energy) of process **I** are very close in the three compounds examined and rotation around the C(sp^3)–C(sp^3) bond does not seem to differ significantly as a function of the different aryl groups. For process **II** larger experimental errors affect the activation parameters, yet the energy of activation and enthalpy of activation is lower in compound **3**. Probably, in this compound the transition state, where the bulky –CCl$_2$Ar group is eclipsed with the pyridine ring, is partly stabilized by electrostatic interactions between the negative chlorine atoms and the electron-deficient heterocyclic ring. The importance of transition state structure in determining the height of the rotational barrier is suggested by the fact that in benzylidene dichloride the ground state is of **A** type[5] and the barrier for rotation of the –CHCl$_2$ group is very low,[4,5] *ca.* 2 kcal mol^{-1}, and increases[6,7] to *ca.* 14 kcal mol^{-1} when two *ortho* substituents are inserted in the molecule. In compounds **1–3** the ground state is of **B** type, no *ortho* substituents are present yet the increase of *ca.* 6 kcal mol^{-1} of the barrier with respect to benzylidene dichloride should be determined entirely by the bulk of the –CCl$_2$Ar group which, in the transition state, is coplanar with the aromatic ring, as is also shown by the theoretical results.

The entropy of activation found experimentally is positive as measured also previously[8] for process **I** in 2,2,3,3-tetrachloro-butane. The effect of condensed media on the conformational equilibria in compounds **1–3** needs further comment. The results of the calculations have shown that the *anti* conformer is the more stable one for all the compounds examined, in agreement with the conformation found for compounds **3** and **4** in the solid state. In solution, at least in the solvents employed, the *gauche* form is more abundant. The results of AM1/MNDO calculations show that the polarity of the *gauche* conformers is

higher than that of the *anti* partner, Table 7: it should thus be expected that the *anti* conformer, which should prevail for the molecules in the gas phase, increases in solvents of progressively higher permittivity.[27] The *anti* conformer of 2,2,3,3-tetrachloro-butane prevails[8] in solution and the population of the more polar *gauche* form increases in more polar solvents.

An extended study of solvent effects on the conformational equilibria of compounds **1–3** was not performed and measurements in a second solvent, [^{2}H]chloroform, were made only for compounds **2** and **3**. Owing to the low concentration of the solute and to the narrow temperature range spanned, the thermodynamic parameters turned out to be affected by a large experimental error, nevertheless they are close to those obtained in [^{2}H$_6$]acetone solution.

In the less polar solvent the population of the *anti* conformer, reported in Table 1, increases, as predicted.

In conclusion, to the questions established as the aim of the present work the following answers can be given: (i) two processes of internal rotation around single bonds were identified and that with the higher energy barrier is associated with *anti–gauche* conformer interconversion; (ii) a second internal process is frozen at lower temperature associated with internal rotation around the C(sp^3)–C(sp^2) bond; (iii) internal rotation of the aromatic rings should have a higher barrier (1–1.5 kcal mol^{-1} from theoretical predictions) in the *gauche* conformer than in the *anti* one; (iv) owing to the difference of energy of activation, *ca.* 6 kcal mol^{-1}, between processes **I** and **II** they can be considered, in a good approximation, as separate processes, and in process **II** only one ring at a time is involved in internal rotation; (v) the rotational ground-states have been characterized: their structures in solution coincide with those of the free molecules and one of them is identical to that found for these molecules in the solid state.

References

1 K. Onuma, Y. Yamashita and H. Hashimoto, *Bull. Chem. Soc. Japan*, 1970, **43**, 836; T. A. Cooper and T. Takeshita, *J. Org. Chem.*, 1971, **36**, 3517; T. Shirafuji, Y. Tamamoto and H. Nozaki, *Bull. Chem. Soc. Japan*, 1971, **44**, 1994; K. Onuma, Y. Yamashita and H. Hashimoto, *Bull. Chem. Soc. Japan*, 1973, **46**, 333.
2 A. Cornia, U. Folli, S. Sbardellati and F. Taddei, *J. Chem. Soc., Perkin Trans. 2*, 1993, 1847.
3 U. Folli, S. Sbardellati and F. Taddei, unpublished results.
4 M. K. Ahmed, D. J. Swanton and B. R. Henry, *J. Phys. Chem.*, 1987, **91**, 293.
5 T. Schaefer and R. Sebastian, *Can. J. Chem.*, 1989, **67**, 2053.
6 A. P. Yatsubov, D. V. Tsyganov, L. I. Belen'kii, V. S. Bogdanov, B. I. Ugrak and M. M. Krayushkin, *Tetrahedron*, 1991, **47**, 5237.
7 M. Oki, *Applications of Dynamic NMR Spectroscopy to Organic Chemistry*, VCH, Weinheim, 1985, p. 201.
8 B. L. Hawkins, W. Bremser, S. Borcic and J. D. Roberts, *J. Am. Chem. Soc.*, 1971, **93**, 4472.
9 A. C. T. North, D. C. Phillips and F. S. Mathews, *Acta Crystallogr., Sect. A.*, 1968, **24**, 351.
10 G. M. Sheldrick, SHELX86: *Program for Crystal Structure Solution*, University of Göttingen, Germany, 1986.
11 G. M. Sheldrick, SHELX76: *Program for Crystal Structure Determination*, University of Cambridge, England, 1976.
12 D. A. Klier and G. Binsch, DNMR3: *A Computer Program for the Calculation of Complex Exchange-Broadened NMR Spectra. Modified Version for Spin Systems Exhibiting Magnetic equiva-*

lence or Symmetry, Program 165, Quantum Chemistry Program Exchange, Indiana University, USA, 1970.

13 C. B. LeMaster, C. L. LeMaster and N. S. True, *Documentation of Changes to DNMR5 for DOS-Based Personal Computers and VAX 11/750*. QCPE Program QCMP 059. Quantum Chemistry Program Exchange, Indiana University, USA, 1989.

14 D. S. Stephenson and G. Binsch, DNMR5: *Iterative Nuclear Magnetic Resonance Program for Unsaturated Exchange-Broadened Bandshapes*, QCPE Program 365, Quantum Chemistry Program Exchange, Indiana University, USA, 1979.

15 G. Binsch, *Top. Stereochem.*, 1968, 3, 97.

16 J. Sandström, *Dynamic NMR Spectroscopy*, Academic Press, London, 1982, p. 81.

17 C. K. Johnson, ORTEP, *Report ORNL-3794*, Oak Ridge National Laboratory, Oak Ridge, Tennessee, 1965.

18 J. Garbarczyk and M. Krolikowska, *Z. Crystallogr.*, 1992, 198, 320.

19 S. Hovmöller, G. Smith and C. H. L. Kennard, *Acta Crystallogr., Sect. B*, 1978, 34, 3016, and refs. therein.

20 F. H. Allen, O. Kennard, D. G. Watson, L. Brammer, A. G. Orpen and R. Taylor, *J. Chem. Soc., Perkin Trans. 2*, 1987, S1.

21 M. J. S. Dewar, E. G. Zoebisch, E. F. Healy and J. J. P. Stewart, *J. Am. Chem. Soc.*, 1985, 107, 3902.

22 W. M. Fabian, *J. Comput. Chem.*, 1988, 9, 369.

23 M. Head-Gordon and J. A. Pople, *J. Phys. Chem.*, 1993, 97, 1147.

24 MOTECC-91. *Modern Techniques in Computational Chemistry*, ed. E. Clementi, International Business Machines Corporation, Kingston, New York 12401, USA, ESCOM, Science Publishers Leiden, 1991.

25 L. Radom and J. A. Pople, *J. Am. Chem. Soc.*, 1970, 92, 4786.

26 GAUSSIAN-92, Revision C: M. J. Frisch, G. W. Trucks, M. Head-Gordon, P. M. W. Gill, M. W. Wong, J. B. Foresman, B. G. Johnson, H. B. Schlegel, M. A. Robb, E. S. Replogle, R. Gomperts, J. L. Andres, K. Raghavachari, J. S. Binkley, C. Gonzalez, R. L. Martin, D. J. Fox, D. J. Defrees, J. Baker, J. J. P. Stewart and J. A. Pople, Gaussian Inc., Pittsburg PA, 1992.

27 P. Hobza and R. Zaharadnik, *Weak Intermolecular Interactions in Chemistry and Biology*, Elsevier, Amsterdam, 1980; R. J. Abraham and E. Bretschneider, in *Internal Rotation in Molecules*, ed. W. J. Orville-Thomas, Wiley, London, 1974.